ACS OMEGA

Article

Photoinduced Energy Transfer in ZnCdSeS Quantum Dot–Phthalocyanines Hybrids

Sadananda Mandal,*,† Miguel Garcia Iglesias,‡,§ Mine Ince,‖,⊥ Tomás Torres,‡,§,# and Nikolai V. Tkachenko*,†

†Laboratory of Chemistry and Bioengineering, Tampere University of Technology, P. O. Box 541, 33101 Tampere, Finland
‡Departamento de Química Orgánica, Universidad Autónoma de Madrid, Cantoblanco, E-28049 Madrid, Spain
§IMDEA-Nanociencia, C/Faraday, 9, Cantoblanco, 28049 Madrid, Spain
‖Advanced Technology Research & Application Center, Mersin University, Ciftlikkoy Campus, TR-33343 Mersin, Turkey
⊥Department of Energy Systems Engineering, Faculty of Tarsus Technology, Mersin University, 33480 Mersin, Turkey
#Institute for Advanced Research in Chemical Sciences (IAdChem), Universidad Autónoma de Madrid, 28049 Madrid, Spain

Ⓢ Supporting Information

ABSTRACT: In this article, interaction between ZnCdSeS quantum dot (QD) and phthalocyanines with variable linker has been reported. Steady-state and time-resolved spectroscopic investigation reveals that only photoinduced energy transfer occurs from QD to phthalocyanines. To evaluate quantitatively the energy transfer, the Poisson statistics of QD−dye complex formation was used in the analysis of steady-state and time-resolved emission quenching, which allows to estimate the energy transfer rate constant for an ideal one-to-one complex. The measured rate constants are compared to the rates evaluated based on the classic Förster theory, which shows roughly 1 nm discrepancy in the energy transfer distance estimation, or one order in magnitude discrepancy in the transfer rate constants.
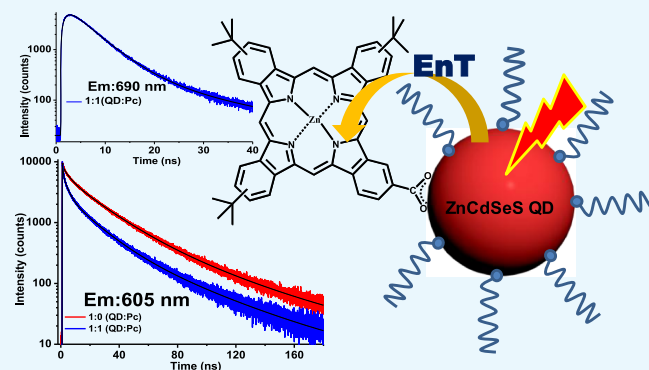
1. INTRODUCTION

In the last few decades, semiconductor quantum dots (QDs) have gained growing interests due to their advanced photophysical properties, versatile functionalities, and wide range of applications in solar cells, optoelectronic devices, and sensors.[1−3] Besides, core and core−shell type QDs, alloyed QDs have also attracted attention because of their tunable optical properties by varying the composition of the QDs without changing the particle's size.[4−6] It has been reported that the alloyed QDs such as ZnCdSe QDs without shell have better charge injection ability compared to those CdSe/ZnS core−shell QDs.[7] Even, more advanced photophysical properties can be achieved by combining QDs with organic dyes to form QD−dye hybrids for the benefits of both components in a single architecture.[8−12] A large number of research works has been reported on QD−dye hybrids with two types of photoinduced interactions, namely, energy transfer and charge transfer, and there are few examples of QD−dye hybrids where competition between these two reactions was observed.[8,13−21] In QD−dye hybrids, QDs act as perfect energy donors because of their extended absorption spectra and high extinction coefficient, whereas higher conductance band (CB) energy of QDs compared to lowest unoccupied molecular orbital (LUMO) of various dyes may also favor a competing charge

transfer process upon excitation of QDs. However, quantitative characterization of either of the processes, energy and charge transfer, remains a challenging task.[19,22] Although Förster-type resonance energy transfer is a common approach to analyze energy transfer in QD−organic dye hybrids, the quantitative analysis is complicated by the statistical nature of hybrid formation and inhomogeneity of QD properties observed as essentially nonexponential decay of emission of pure QDs.[12,22] There are also reports on unusual distance dependence on the energy-transfer efficiency on the length of linker connecting QD and energy acceptor.[13]

An important advantage of QD−dye hybrid is the relative ease of hybrid fabrication. Organic dyes with proper binding groups can easily form the complexes spontaneously in the solutions.[23] Though the downside of this advantage is that it is impossible to control the number of dyes attached to a single QD, or inherent statistics of the hybrid formation.

Among the various organic dye molecules, phthalocyanines are outstanding for light harvesting due to their high molar absorption coefficient in the red−near-infrared region and high

thermal as well as chemical stability.[24,25] They have already shown potential applications in various fields such as solar cell, photodynamic therapy, and infrared sensors.[26−30] Therefore, QD−phthalocyanine hybrids with advanced properties would be excellent materials for solar energy conversion. Lee et al. showed that PbS QD−carboxyphthalocyanine (TT1) composite in solid state had high efficiency for panchromatic harvesting of light.[11] There are few examples of QD−phthalocyanine hybrids, where efficient energy transfer or charge transfer was observed from QD to phthalocyanine.[31−34] Recently, our group reported an ultrafast charge transfer from photoexcited CdSe QD to free base phthalocyanine.[34] However, photophysics of the hybrids was affected by phthalocyanine aggregation and no interaction between QD and phthalocyanine was observed when the phthalocyanine counterpart was excited. Up to date, it is well known that energy transfer may occur from QD to phthalocyanines; however, the factors affecting energy transfer rate and efficiency are not well understood.

In the present study, we investigated the photophysical interactions between ZnCdSeS QD (core without shell, good electron/energy donor) and three different phthalocyanines (TT1, TT3, and TT6) in QD−phthalocyanine hybrids. The CB energy of QD is higher than that of LUMOs of phthalocyanines, which thermodynamically favors the electron transfer from QD to phthalocyanine. However, it has been observed that only efficient energy transfer occurred from QD to phthalocyanines. The energy transfer from QD to three different phthalocyanines, depending on the length of linker and aggregation of the phthalocyanines, has been investigated using steady-state and time-resolved spectroscopy. Poisson statistics was employed to obtain quantitative information on the energy transfer rate constants in ideal one-to-one QD−phthalocyanine hybrids. The rate of energy transfer was also calculated based on the Förster model accounting for hybrid geometry and measured emission and absorption spectra of the energy donor and acceptor. Comparison of the measured and calculated rate constants indicates that the direct application of the Förster theory may lead to erroneous results.

2. RESULTS

2.1. Differential Pulse Voltammetry (DPV) Measurement. The DPV measurements were carried to estimate the valence band (VB) and conductance band (CB) energy of the QD and highest occupied molecular orbital (HOMO)−LUMO energies of the phthalocyanines. Figure 1 shows the DPV curves of TT1 (see the Supporting Information (SI), Figure S1 for the DPV curves of QD and TT3 and TT6). The estimated VB of the QD is −4.68 eV vs vacuum level and considering the absorption peak of QD, the CB is −2.60 eV vs vacuum level. The TT1 HOMO and LUMO energies relative to vacuum level are −4.71 and −3.06 eV, respectively. It is to be noted that the corresponding HOMO−LUMO of TT3 and TT6 are roughly same as that of TT1, as expected (detailed calculation of DPV of QD and three phthalocyanines are given in the SI). Because the LUMOs of phthalocyanines have lower energy than the CB of QD, there is a possibility of electron transfer from QD to phthalocyanines upon the excitation of QD.

2.2. Steady-State Absorption and Evidences for Aggregation at High Concentrations. Absorption spectra of QD and QD−phthalocyanine complexes were measured at a constant concentration of QD and different concentrations of
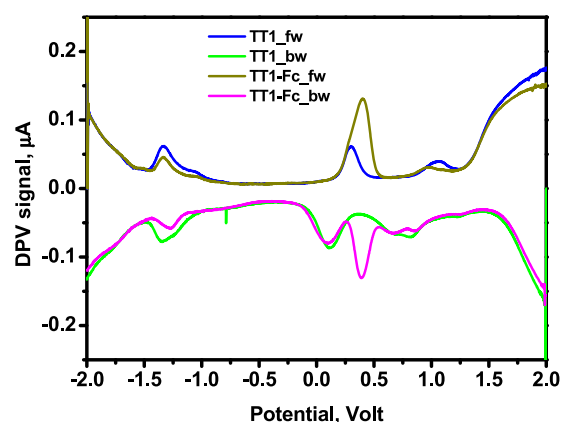

Figure 1. Differential pulse voltammogram of TT1: fw, forward scan; bw, backward scan; Fc, ferrocene.

phthalocyanine. Figure 2A shows the absorption spectra of QD and different molar ratios QD/TT1 of the hybrids. Interestingly, TT1 is poorly soluble in hexane and becomes aggregated, but the carboxylic acid group of the TT1 has a stronger binding to ZnCdSeS surface than amine,[35] and in the presence of QD, TT1 replaces the amine ligands at/on the QD surfaces to form the complex and to place itself between alkyl tails of the ligands, which precludes the aggregation of TT1 at least at low TT1 relative concentrations. In the absence of QD, same concentration of TT1 shows different absorption spectra with very low absorbance value in hexane compared to QD−TT1 complex (see the SI, Figure S2), which is an indication of the QD−TT1 complex formation. Similarly, QD−TT3 and QD−TT6 hybrids are also formed.

A careful examination of the absorption spectra shows that as relative concentration of TT1 in QD−TT1 hybrids increases, the optical density of TT1 increases but not in direct proportion at the higher concentration of TT1. It may be due to the aggregation of TT1 on the QD surface. To clarify this point, absorption spectra of TT1 have been normalized after the subtraction of QDs absorption from QD−TT1 hybrids (depicted in Figure 2B). The spectra have the same shapes up to QD/TT1 = 1:2 ratios, but the relative absorption in the wavelength region of 600−650 nm is higher for 1:5 and 1:10 samples compared to 1:1 and 1:2 hybrids. This observation implies that there is no detectable aggregation of TT1 in QDs−TT1 complex at relative TT1 concentration upto 1:2, but some aggregation features appear at ratio 1:5 and higher.

Figure 2C compares the spectra of TT1 in THF solvent (good solvent for TT1) and 1:1 complex after the subtraction of QD absorption. Only a minor shift in the Q-band absorption was observed for the QD−TT1 hybrid, but the bandwidth stays essentially unchanged. A small spectral shifting may be due to the difference in the environment and the complex formation through the interaction between carboxylic group of TT1 and QDs surfaces. Compared to the QD−TT1 hybrids, some minor aggregation features can be noticed for TT3 and TT6 samples already in the 1:2 complexes with QDs (see the Supporting Information, Figure S3 for QD−TT3 and Figure S4 for QD−TT6). It may be due to the variation in linker between the carboxylic acid group and the main skeleton of the phthalocyanines. In the case of TT1, carboxylic group is directly attached to the main skeleton of
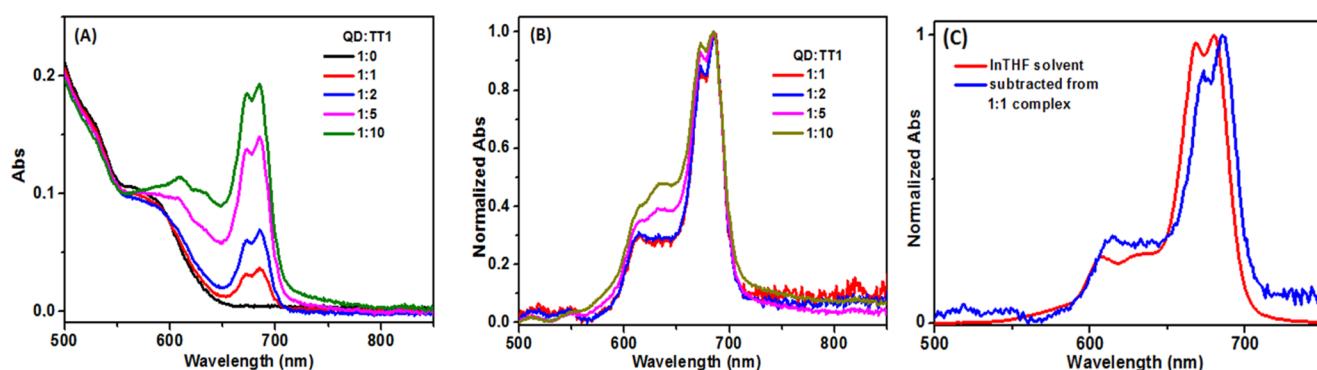
Figure 2. (A) Absorption spectra of QD and QD−TT1 hybrids. (B) Normalized absorption spectra of TT1 after the subtraction of QD absorption. (C) Normalized absorption spectra of TT1 in tetrahydrofuran (THF) and in QD−TT1 hybrid.
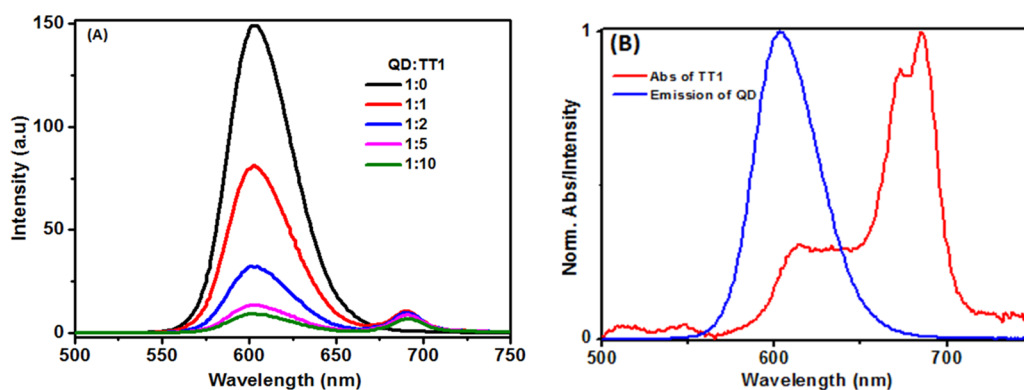
Figure 3. (A) Emission spectra of QD and QD−TT1 hybrids and (B) overlap between absorption spectrum of TT1 and emission spectrum of QD.
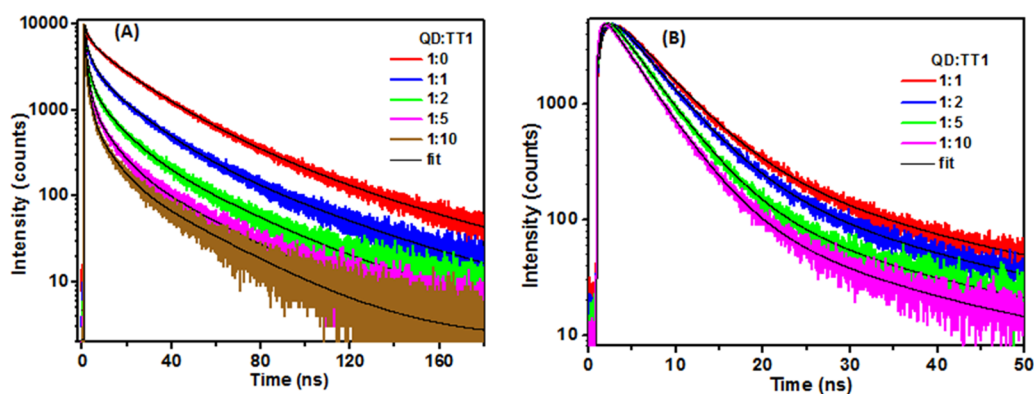
Figure 4. Emission decay curves of QD and QD−TT1 complexes at the excitation wavelength of 405 nm and monitoring emission wavelengths of (A) 605 nm and (B) 690 nm.

the phthalocyanine, whereas TT3 and TT6 contain carboxylic group with ethylene and phenyl linker, respectively.

2.3. Steady-State Emission Quenching. The emission spectra of QD and QD−TT1 hybrid with different ratios are shown in Figure 3A. Increase in TT1 concentration leads to a decrease in the emission intensity of QDs. The plausible reasons for the fluorescence quenching of QD in the presence of TT1 are (a) electron transfer between QD and TT1, (b) energy transfer from QD to TT1, and (c) both electron and energy transfer. It is seen that there is good overlap (shown in Figure 3B) between the absorption spectrum of TT1 (after the subtraction of absorption of QD from 1:1 QD−TT1 complex) and emission spectrum of QD with the overlap integral value of 2.49×10^{-13} M^{-1} cm^3, indicating the possibility of energy transfer from QD to TT1. Furthermore, in addition to the

fluorescence quenching of QD in the QD−TT1 complex, there is a formation of new emission peak at 690 nm, which is assigned tentatively to energy-transfer-mediated TT1 fluorescence.

The emission spectra of QD, QD−TT3, and QD−TT6 have also been measured (see the SI, Figure S5). The fluorescence quenching of QD was observed and has essentially similar trend for QD−TT3 and QD−TT6 hybrids. The calculated overlap integral values are 4.05×10^{-13} and 5.63×10^{-13} M^{-1} cm^3 for TT3 and TT6, respectively (the absorption spectra of TT3 and TT6 were taken from their respective 1:1 complex, and the overlap spectra are given in the SI Figure S6). The overlap integrals were calculated based on the molar absorption of the phthalocyanines in hybrids and normalized emission spectrum of QD. The molar absorption of

Table 1. Emission Decay Fit Parameters of QD and QD−TT1 Hybrids, the Time Constants, τ_i, Corresponding Pre-exponential Factors, a_i, and the Average Lifetime, $\langle\tau\rangle^a$

QD/TT1	τ_1 (ns) (a_1)	τ_2 (ns) (a_2)	τ_3 (ns) (a_3)	τ_4 (ns) (a_4)	$\langle\tau\rangle^a$ (ns)
1:0	0.5 (0.27)	4.5 (0.22)	20.9 (0.41)	51.6 (0.10)	14.8
1:1	0.4 (0.44)	3.3 (0.31)	16.6 (0.21)	46.0 (0.05)	7.0
1:2	0.2 (0.55)	2.1 (0.30)	10.7 (0.11)	34.8 (0.04)	3.3
1:5	0.2 (0.58)	1.7 (0.32)	8.0 (0.08)	31.5 (0.02)	1.9
1:10	0.2 (0.61)	1.5 (0.31)	7.2 (0.06)	30.5 (0.02)	1.6

^{a}Standard deviations are in the range 4−10%.
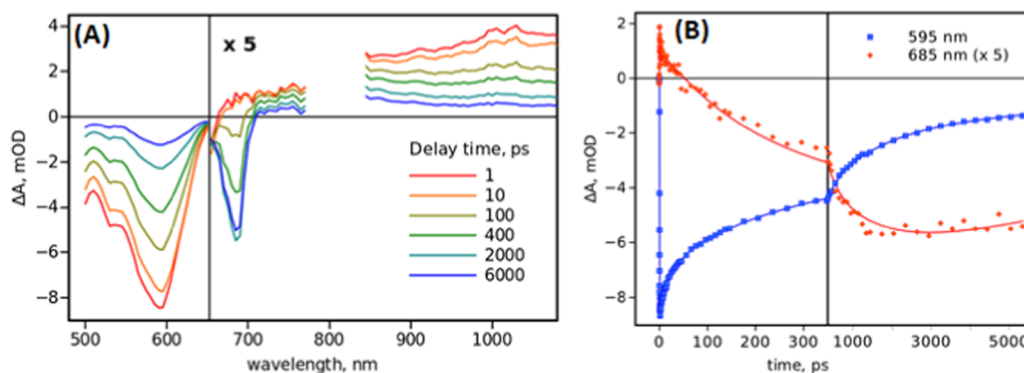
Figure 5. (A) Time-resolved transient absorption spectra of QD/TT1 hybrids at a few delay times (indicated in the plot) after excitation at 480 nm. The responses at >650 nm are multiplied by five for a better visibility. (B) Transient absorption profiles at 595 and 685 nm, which correspond to lower-energy absorption band of QD and strongest Q-band of Pc, respectively.

phthalocyanines were evaluated from the phthalocyanine absorption spectra in hybrids after subtracting the absorption of QDs, as presented in Figure 2B, and thus accounts for the specific phthalocyanine environment in the hybrid (including possible aggregation effects). The overlap integral values increase the in order TT1 < TT3 < TT6, though the values are reasonably close to each other. The difference may be due to minor structural differences in the phthalocyanines and somewhat higher aggregation of TT3 and TT6 than that of TT1 on the QD surface. It is to be noted that quantitative evaluation of the aggregation degree is complicated because the types of aggregates, their spectra, and molar absorption are not known.

2.4. Emission Decays. Time-correlated single photon counting (TCSPC) was used to determine the emission lifetimes of QD and different QD−phthalocyanine hybrids. The samples were excited at 405 nm, which selectively excites QD (negligible absorption of phthalocyanine at this wavelength), and emission was monitored at 605 nm (emission of QD) and 690 nm (emission of phthalocyanine). Figure 4A shows the emission decay curves of QD and the corresponding QD−TT1 hybrids at the monitoring wavelength of 605 nm. It is to be noted that even the emission decay of pure quantum dot is not monoexponential. A multiexponential decay model has been used to obtain a reasonable fit. In addition to the individual lifetime components, average lifetimes of the QD and corresponding hybrids have been calculated and summarized in Table 1. It has been observed that the lifetime of the QD decreases with the increasing concentration of TT1, consistent with the similar trend observed in the fluorescence intensity quenching. Emission decays of QD−TT3 and QD−TT6 hybrids (see the SI, Figure S7 for emission decay curves and Tables S1 and S2 for fit decay parameters) follow the similar trend as expected.

The emission decay curves of QD−TT1 hybrids at the monitoring wavelength of 690 nm are shown in Figure 4B. The emission decay curves were fitted by triexponential model and the fastest components had negative pre-exponential factors, indicating a rise in emission (for fitting parameters, see the SI, Table S3). Rising components have also been observed in the case of QD−TT3 and QD−TT6 hybrids (emission decay curves are given in the SI, Figure S7B,D for QD−TT3 and QD−TT6, respectively).

2.5. Transient Absorption (TA) Spectroscopy. Time-resolved TA spectroscopic measurements of QD and QD−Pc hybrids were carried out using femtosecond pump−probe system. The transient absorption response of QD suspension at the excitation wavelength of 480 nm is shown in the SI, Figure S8.

At delay times of 1 ps and longer, it mainly shows bleaching of the lower-energy absorption band of QD, which recovers slowly in hundred picosecond to ten nanosecond time domain. Addition of TT1 does not change the transient absorption response at short delay times, <10 ps, but changes the response gradually at long delays (Figure 5). At the qualitative level, there is a clear bleaching of the TT1 absorption around 685 nm, which develops in a few hundred picosecond time. There is also some change in the near-IR transient absorption spectrum shape, it becomes "flatter". However, there is no evidence of any cation or anion formation during the photoexcitation relaxation. The details of the TA spectra fitting, discussion, and few more TA spectra can be found in the SI, Figures S9−S11.

3. DISCUSSION

3.1. Dependence of Quenching on Concentration. The addition of phthalocyanine solutions into the QD suspension results in quenching of both emission intensity and lifetime of the QDs. The quenching increases with the

increasing concentration of phthalocyanines (calculated quenching efficiency based on average lifetimes are given in the SI, Table S4). The quenching concentration dependence is presented in Figure 6 (for TT3 and TT6 given in the SI, Figure
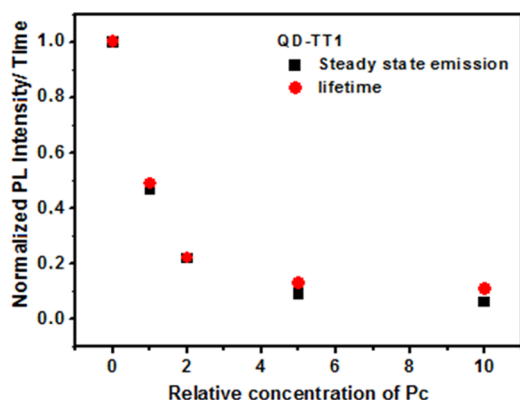
Figure 6. Relative decrease in emission intensity and average lifetime as a function of relative TT1 content for the different QD−TT1 hybrids (standard deviations for calculated average lifetimes are in the range of 4−10%).

S12). At low concentration of TT1, the emission intensity quenching and average lifetime quenching are almost same. However, at higher concentration of TT1, there is a small difference between emission intensity and average lifetime quenching. The difference between emission intensity quenching and average lifetime quenching is somewhat greater in QD−TT3 and QD−TT6 hybrids. This discrepancy originates from the time resolution of the instruments used (roughly 0.1 ps) for lifetime measurements most probably. At higher concentrations, the quenching is faster, and the fast decay is ill resolved at the ratio 1:10.

The plausible mechanisms for the quenching of QD are charge transfer (CB energy of QD is higher compared to the LUMOs of the phthalocyanines) and energy transfer (good overlap between the absorption spectrum of phthalocyanine and emission spectrum of QD). However, the emission at phthalocyanine fluorescence wavelength (emission intensity of QD−Pc at 690 nm is higher than that of Pc in THF with the same concentration of Pc, see the SI, Figure S13A), and more importantly the presence of the rising component at the emission wavelength of the phthalocyanine fluorescence, 690 nm (emission decay of TT1 in THF at 405 nm excitation is also given in the SI Figure S13B for comparison), indicate that the energy transfer takes place from QDs to phthalocyanine. This is also confirmed by the transient absorption spectroscopy studies showing no characteristic features (for example, occurrence of radical cations of electron donor and radical anion of electron acceptor) of charge transfer from QD to phthalocyanine or phthalocyanine to QD in the QD−phthalocyanine hybrids, but is consistent with energy transfer (slow rise of phthalocyanine ground state absorption bleaching around 690 nm). Therefore, the charge transfer process is ruled out in this system, and we can focus on our analysis of the QD emission quenching on the energy transfer. It is to be noted that the energy-transfer analysis based on the rise time of phthalocyanine energy acceptor is more complicated and less accurate. The emission intensity at 690 nm is much weaker compared to that at 605 nm (see the SI, Figure S14), and the decay profile depends on the lifetime of the phthalocyanine

energy acceptor, which interferes with the energy transfer time constant.

It is usually assumed that at nanometer distances, the energy transfer follows the Förster resonance energy transfer (FRET) model. In general, FRET is a process involving the non-radiative energy transfer from a "donor" fluorophore to an appropriate "acceptor" counterpart. This process arises from the dipole−dipole interactions and strongly depends upon the center-to-center distance of the corresponding energy donor and acceptor. According to the Förster theory, the rate constant of the energy transfer for an isolated single donor−acceptor pair separated by a distance r is given by the following equation[36]

$$k_T(r) = \frac{1}{\tau_D}\left(\frac{R_0}{r}\right)^6 \tag{1}$$

where τ_D is the lifetime of the donor in the absence of the acceptor and R_0 is known as the Förster distance, the distance at which the transfer rate constant $k_T(R_0)$ is equal to the excited state decay rate constant of the donor in the absence of acceptor. The Förster distance (R_0) can be estimated as

$$R_0 = \frac{9000(\ln 10)\kappa^2 \phi_D}{128\pi^5 N n_0^4} J(\lambda) \tag{2}$$

where ϕ_D is the quantum yield of donor in the absence of acceptor, N is the Avogadro's number, n_0 is the refractive index of medium, and κ^2 is the orientation factor of two dipoles interacting. The value of κ^2 depends on the relative orientation of the donor and the acceptor dipoles. For randomly oriented dipoles, $\kappa^2 = 2/3$, which varies between 0 and 4 for the cases of orthogonal and parallel dipoles, respectively. $J(\lambda)$ is the spectral overlap integral, which is defined as

$$J(\lambda) = \int_0^\infty F_D(\lambda)\varepsilon_A(\lambda)\lambda^4 d\lambda \tag{3}$$

where $F_D(\lambda)$ is the normalized emission spectrum of donor, $\varepsilon_A(\lambda)$ is the molar absorption coefficient of acceptor at the wavelength λ (in nm). The calculated R_0 for QD−TT1, QD−TT3, and QD−TT6 hybrids are 40, 44, and 46 Å, respectively.

3.2. Poisson Distribution of Pc in Hybrid. To analyze the emission intensity as well as the average lifetime quenching of QD in QD−Pc hybrids, we can assume that the simultaneous formation of hybrids with different QD−Pc ratios is described reasonably well by Poisson statistics[15,37,38]

$$P_n = \frac{c^n}{n!}e^{-c} \tag{4}$$

where n is the number of phthalocyanine molecules in the hybrid, P_n is the probability to find a hybrid with n phthalocyanines, and c is the relative molar concentration of phthalocyanines in the sample solutions, as denoted in Figures 2−6.

To model QD emission decays, one can use the Poisson statistics of the hybrid formation and sum up the decays of QDs with different number of phthalocyanines and thus having different quenching rate constants, which was shown to yield[15]

$$A(t, c) = A_0 \exp\left[\frac{-t}{\tau_0} - c\left(1 - \exp\left(\frac{-t}{\tau_{ET}}\right)\right)\right] \tag{5}$$
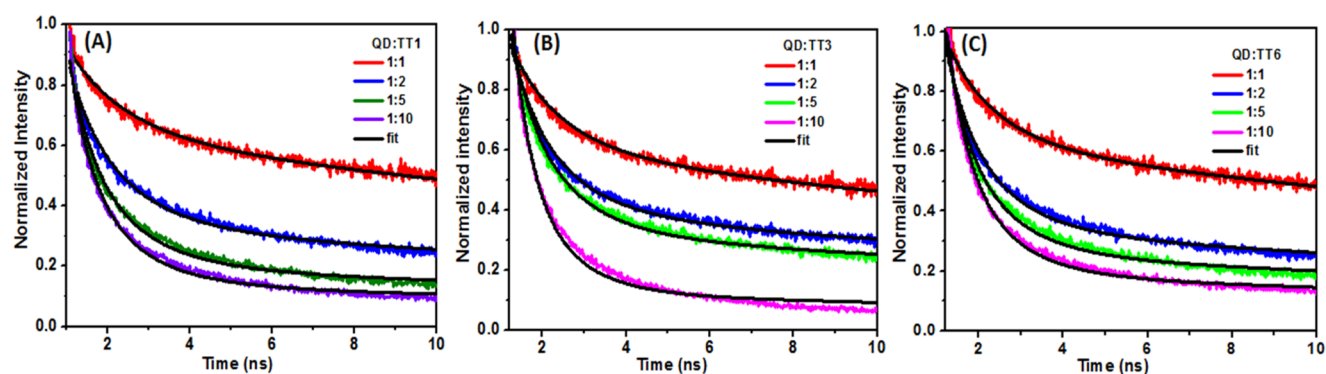
Figure 7. Emission decays of QD−phthalocyanine hybrids normalized by emission decays of QD and fitted by Poisson distribution model: (A) QD−TT1, (B) QD−TT3, and (C) QD−TT6.

Table 2. Fitted Parameters (Using Poisson Distribution Model, eq 5) of QD−Phthalocyanine Hybrids

QD−Pc	τ_0 (ns)	c_1 (A_1)	c_2 (A_2)	c_5 (A_5)	c_{10} (A_{10})	τ_{ET} (ns)
QD−TT1	34	0.38 (0.92)	0.98 (0.88)	1.52 (0.90)	1.89 (0.91)	1.71
QD−TT3	34	0.53 (1.02)	1.02 (1.09)	1.27 (1.17)	2.54 (1.53)	1.49
QD−TT6	34	0.50 (1.04)	1.17 (1.09)	1.50 (1.17)	1.92 (1.29)	1.44

where τ_0 is the lifetime of a nonhybridized QD, τ_{ET} is the energy transfer time constant from the exited QD to single phthalocyanine, c is the relative concentration of phthalocyanines, and A_0 is a constant determined by the initial population of the excited state.

Unfortunately, the decay model of eq 5 cannot be applied directly to the measured decays because the relaxation of excited QD is not monoexponential, which indicates inhomogeneity due to the presence of surface traps and different sort of defects. To overcome the problem of QD inhomogeneity, the hybrid decays were normalized to the decay of pure QD. Then, the fit model of eq 5 was applied simultaneously to all normalized decays at different concentrations of phthalocyanine quencher, which resulted in common τ_0 and τ_{ET} values and a set of relative concentrations for each sample. The fitted curves for QD−phthalocyanines are shown in Figure 7, and the fit results are summarized in Table 2.

It should be noted that strictly speaking the value of τ_0 must be infinitely long in this case because the decays were already normalized to the natural decay of the QDs alone. However, the obtained value is much longer than the time interval used for fitting, 10 ns; therefore, τ_0 can be considered to be sufficiently large. The energy transfer time constant is close to 1.5 ns for all three phthalocyanines, which is shorter than the average lifetimes reported in Table 1 for all samples. According to the model, τ_{ET} is the energy transfer time constant in exactly one-to-one complex, whereas the average lifetime reported in Table 1 accounts for all combinations on hybrids, in which case, QDs without phthalocyanines have a relatively high contribution due to a rather long lifetime of unquenched QDs (because $\tau_0 \gg \tau_{ET}$).

The fit uses concentration, c, as a free parameter, and it comes out that the concentration estimated from the quenching dynamics is two or more times lower than the intended concentration. However, the calculated values for 1:2 hybrids are roughly double compared to that for 1:1. The estimated concentration increases further for 1:5 and 1:10 hybrids, though the relative increase is smaller that expected. This can be explained by the aggregation tendency of the

phthalocyanine used, which leads to a change in absorption spectrum and becomes noticeable for 1:5 and 1:10 samples. The concentration discrepancy at low concentration (1:1 and 1:2 samples) cannot be attributed to the aggregation. In fact, according to the Poisson statistics of the hybrid formation, the relative emission yield of the sample prepared by mixing equal number of QD−phthalocyanines (1:1 sample) is 0.37 if quenching time constant is much shorter than the QD lifetime and 0.42 if the time constants are 1.7 and 34 ns for τ_0 and τ_{ET}, respectively (presumably, the case of QD/TT1 hybrids). The measured value is 0.48, or 15−30% higher than the expected one. This rises the question on the accuracy of the relative concentration estimation based on the absorptions. The most significant source of inaccuracy is the concentration of QDs, which was estimated from the analytical dependence of the QD molar absorption on the size and thus the position of the lowest energy absorption band. The dependence was established for CdSe core-only dots, but alloyed dots were used in this study. This can result in 15−30% systematic error in the QD concentration estimation. Arguably, the estimation made on the basis of Poisson statistics of hybrid formation can be considered as more reliable, as the latter is based on the simultaneous analysis of the whole series of measurements.

Furthermore, we have re-evaluated the QD/Pc ratios accounting for the steady-state emission and emission decay data scaled by 0.85 and plotted theoretical quenching dependence, one presuming $\tau_0 \gg \tau_{ET}$ and another taking $\tau_0 = 34$ ns, $\tau_{ET} = 1.7$ ns, in Figure 8. These results suggest the QD/Pc ratios to be 1:0.85 and 1:1.7 in place of 1:1 and 1:2, respectively. According to this model, the rates of energy transfer are 5.80×10^8, 6.67×10^8, and 7.01×10^8 s^{-1} for QD−TT1, QD−TT3, and QD−TT6 hybrids, respectively, i.e., the rate of energy transfer increases from QD−TT1 to QD−TT6, as expected from the overlap integral value of three different phthalocyanines−QD hybrids.

3.3. Effect of Pc Linker on the Energy Transfer. Because FRET depends on the distance between donor and acceptor, the Pc linker should play an important role in controlling the rate of energy transfer in QD−Pc hybrids. Previously, Dayal et al.[13] reported non-Förster-type energy
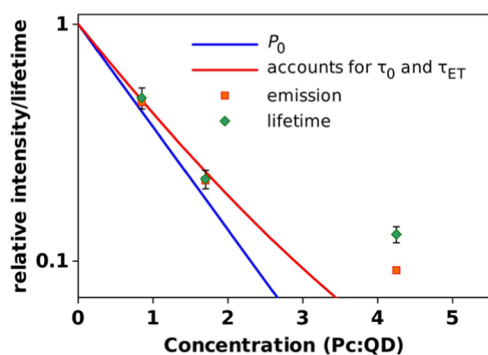
Figure 8. Steady-state emission and emission decay data scaled by QD/Pc = 0.85 and presuming $\tau_0 \gg \tau_{ET}$ (P_0, blue line) and taking τ_0 = 34 ns, τ_{ET} = 1.7 ns (red line, τ_0 is the lifetime of a nonhybridized QD and τ_{ET} is the energy transfer time constant).

transfer (increased energy transfer efficiency for longer linker chain length) in CdSe QD−silicon phthalocyanine conjugates. In this work, the rates of energy transfer and overlap integrals were determined from the experimental results and can be used to calculate the distance between the donor and acceptor, r, within the FRET framework. These experimental r values are 28, 30, and 31 Å for TT1, TT3, and TT6 hybrids, respectively, and presented in Table 3. The center-to-center distance estimated based on the QD radius and assuming that phthalocyanines are standing upright on the QD surface, r_{theor}, are 39, 43, and 42 Å, for TT1, TT3, and TT6, respectively. Based on r_{theor} values, the calculated rates of energy transfer are 7.8×10^7, 7.7×10^7, and 11.6×10^7 s^{-1} for QD−TT1, QD−TT3, and QD−TT6 hybrids, respectively, or almost one order in magnitude slower than the measured values. This strong discrepancy rises the question on the applicability of the classic FRET model to this case. The theory presumes that both donor and acceptor are point dipoles. This approximation is hardly acceptable for the QDs, which have non-negligible size and to some extent can be considered as a surface to which a small energy acceptor is attached. In other words, the electron density distribution in the QD has to be accounted for and cannot be reduced to a point dipole placed in the middle of QD. This was a known issue and, for example, studied for the electronic excitation transfer from polyfluorene to porphyrin,[39] or in layered structures.[40] The practical outcome of their study is that the energy transfer is more efficient in QD−dye hybrids than that predicted on the basis of classic Förster theory with distance measured from the center of QD to the center of dye.

Three phthalocyanines used in this study differs by the linker between carboxyl anchor and chromophore core only. This looks like an ideal platform to study the distance dependence of the energy transfer. Comparison of TT1 and TT3 is the most straightforward in this respect, with the only difference between the two being the phenyl group between the

phthalocyanine core and the carboxyl binding group. Phenyl is a rigid group and one can expect an increase in separation distance by roughly 4 Å in the case of upright orientation of the phthalocyanine on the QD surface. However, the difference in r values is only 2 Å. This can be interpreted in favor of a lower than six order distance dependence. At the same time, one can notice that the orientation of the carboxyl group is different in these two compounds. It is expected to be out of phthalocyanine core plane in TT1 and most probably in-plane in TT3. This means that a tilt of two Pcs can be very different and alternative explanation of the small difference is a larger tilt angle of TT3 compared to that of TT1.

The most surprising result in the series is that according to the relation between the energy transfer rates of three phthlocyanines, TT6 is spaced further away from QD than two other phthalocyanines. It seems that TT6 has the most upright orientation on the surface. Though the difference between the three studied compounds is relatively minor and can be well explained by minor differences in orientations or factor κ^2 in eq 2.

4. CONCLUSIONS

In summary, we have investigated the energy transfer from ZnCdSeS QD to three different phthalocyanines. Poisson statistical model has been employed to evaluate the concentration ratio of QD−Pc hybrids and to extract the energy transfer rate constants in ideal one-to-one QD−dye complexes. The rates are compared with those calculated using a traditional Förster energy transfer theory, and we show that the theory underestimates the energy transfer rate by roughly an order in magnitude. Our interpretation is that the point dipole approximation is oversimplification in the case of quantum dots, and a suitable theory must take into account the physical size of the QD and probably the electron density distribution close to the QD surface.

5. METHODS AND MATERIALS

ZnCdSeS-alloyed quantum dots were purchased from PlasmaChem GmbH. According to the manufacturer, the quantum dots are spherical with the diameter of 6 nm. The quantum dots are capped with oleyl amine and dispersible in nonpolar organic solvents. The QDs with the emission wavelength of 610 ± 5 nm were used in this study. The quantum yield of the QD was 10% and determined using rhodamine 6G as a standard reference dye.

Three different phthalocyanines (TT1, TT3, and TT6) were utilized in this work. The molecular structures of these phthalocyanines have been given in Scheme 1 and the synthesis of these phthalocyanines (Pc) have been described elsewhere.[41−43]

The supplied QDs (in powder form) were dispersed in hexane and solutions of phthalocyanines were prepared in

Table 3. Calculated Parameters of Energy Transfer[a]

QD/Pc	$J(\lambda)$ (M^{-1} cm^3)	R_0 (Å)	r (Å)	k_{ET} (s^{-1})	r_{theor} (Å)	k_{ETT} (s^{-1})
QD−TT1	2.49×10^{-13}	40	28	5.8×10^8	39	0.78×10^8
QD−TT3	4.05×10^{-13}	44	30	6.76×10^8	43	0.77×10^8
QD−TT6	5.36×10^{-13}	46	31	7.01×10^8	42	1.16×10^8

[a]r is the distance between donor and acceptor (center-to-center) calculated from Poisson distribution model and measured energy transfer rate constants, r_{theor} is the theoretical or geometric donor−acceptor center-to-center distance, and k_{ETT} is the rate constant calculate form the Förster theory and assuming distance r_{theor}.

Scheme 1. Molecular Structures of TT1, TT3, and TT6 and Schematic Presentation of TT1−QD Hybrid
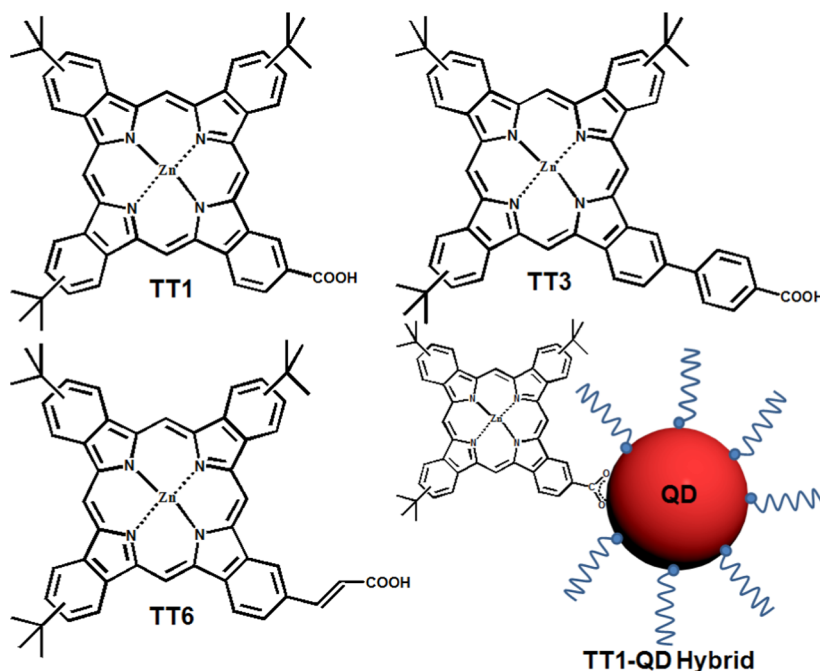
tetrahydrofuran (THF). The QD−Pc complexes were prepared by the addition of microliter amount of Pc solution into the QD solution under vigorous stirring. Different ratios of QD/Pc (1:1 to 1:10) were prepared by adding different amount of phthalocyanine solution.

The differential pulse voltammetry (DPV) technique was used to estimate the oxidation and reduction potentials of QD, TT1, TT3, and TT6 using a Ag/AgCl wire as a pseudoreference electrode. Tetra-butylammonium hexafluorophosphate (TBAPF$_6$), 0.1 M, in chloroform was used as the supporting electrolyte. After measuring the background, a chloroform solution of each sample was added to the electrochemical cell. To fix the reference potential, the measurements were repeated after adding ferrocene (in chloroform) solution for each sample. The measurements were carried out under a nitrogen flow in two directions: toward the positive and the negative potential. The final values of oxidation and reduction potentials were calculated as an average of the two scans relative to a ferrocene standard as reference.

The UV−vis absorption spectra of QDs and QD−Pc complexes were measured with a Shimadzu UV-3600 UV−vis−NIR spectrophotometer. The fluorescence emission spectra were recorded with an ISA-Jobin Yvon-SPEX-Horiba Fluorolog-3-111 fluorophotometer. The raw signals were corrected using an instrument response function provided by the manufacturer. The fluorescence lifetimes of the samples were measured using a time-correlated single photon counting (TCSPC) system by PicoQuant GmbH. The TCSPC system consists of a PicoHarp controller and a PDL-800B driver. The samples were excited by a pulsed laser diode (LDH-P-C-405) at 405 nm. The fluorescence decays were monitored at the emission maxima of quantum dots and emission maxima of phthalocyanines. The time resolution of the TCSPC system was approximately 60 ps (full width at half-maximum).

A description of the pump−probe instrument used in this work is provided in the Supporting Information (SI).

ASSOCIATED CONTENT

Ⓢ Supporting Information

The Supporting Information is available free of charge on the ACS Publications website at DOI: 10.1021/acsomega.8b01623.

> DPV data of QD, TT3, and TT6 and calculations, steady-state and time-resolved spectra of QD, QD−TT3, and QD−TT6 and fit parameters, transient absorption description, time-resolved TA spectra and fitted data with discussion, emission, and decay time decrease comparison data of QD−TT3 and QD−TT6, steady-state and time-resolved comparison data of QD−TT1 and TT1 in THF, emission decays at excitation 405 nm and at different monitoring wavelengths (PDF)

AUTHOR INFORMATION

Corresponding Authors
*E-mail: sadananda.mandal@tut.fi (S.M.).
*E-mail: nikolai.tkachenko@tut.fi (N.V.T.).

ORCID Ⓘ
Sadananda Mandal: 0000-0002-4368-7047
Miguel Garcia Iglesias: 0000-0001-6359-9020
Tomás Torres: 0000-0001-9335-6935
Nikolai V. Tkachenko: 0000-0002-8504-2335

Notes
The authors declare no competing financial interest.

ACKNOWLEDGMENTS

■ REFERENCES

(1) Kamat, P. V. Quantum Dot Solar Cells. The Next Big Thing in Photovoltaics. *J. Phys. Chem. Lett.* **2013**, *4*, 908−918.

(2) Guzelturk, B.; Martinez, P. L. H.; Zhang, Q.; Xiong, Q.; Sun, H.; Sun, X. W.; Govorov, A. O.; Demir, H. V. Excitonics of Semiconductor Quantum Dots and Wires for Lighting and Displays. *Laser Photonics Rev.* **2014**, *8*, 73−93.

(3) Lou, Y.; Zhao, Y.; Chen, J.; Zhu, J.-J. Metal Ions Optical Sensing by Semiconductor Quantum Dots. *J. Mater. Chem. C* **2014**, *2*, 595−613.

(4) Bailey, R. E.; Nie, S. Alloyed Semiconductor Quantum Dots: Tuning the Optical Properties without Changing the Particle Size. *J. Am. Chem. Soc.* **2003**, *125*, 7100−7106.

(5) Zheng, Y.; Yang, Z.; Ying, J. Y. Aqueous Synthesis of Glutathione-Capped ZnSe and $Zn_{1−x}Cd_xSe$ Alloyed Quantum Dots. *Adv. Mater.* **2007**, *19*, 1475−1479.

(6) Mandal, S.; Rahaman, M.; Sadhu, S.; Nayak, S. K.; Patra, A. Fluorescence Switching of Quantum Dot in Quantum Dot−Porphyrin−Cucurbit [7] Uril Assemblies. *J. Phys. Chem. C* **2013**, *117*, 3069−3077.

(7) Caruge, J. M.; Halpert, J. E.; Wood, V.; Bulović, V.; Bawendi, M. G. Colloidal Quantum-Dot Light-Emitting Diodes with Metal-Oxide Charge Transport Layers. *Nat. Photonics* **2008**, *2*, No. 247.

(8) Boulesbaa, A.; Issac, A.; Stockwell, D.; Huang, Z.; Huang, J.; Guo, J.; Lian, T. Ultrafast Charge Separation at CdS Quantum Dot/ Rhodamine B Molecule Interface. *J. Am. Chem. Soc.* **2007**, *129*, 15132−15133.

(9) Song, H.; Reed, M. A.; Lee, T. Single-Molecule Devices: Single Molecule Electronic Devices. *Adv. Mater.* **2011**, *23*, No. 1576.

(10) Leck, K. S.; Divayana, Y.; Zhao, D.; Yang, X.; Abiyasa, A. P.; Mutlugun, E.; Gao, Y.; Liu, S.; Tan, S. T.; Sun, X. W.; et al. Quantum Dot Light-Emitting Diode with Quantum Dots Inside the Hole Transporting Layers. *ACS Appl. Mater. Interfaces* **2013**, *5*, 6535−6540.

(11) Lee, H.; Leventis, H. C.; Moon, S.-J.; Chen, P.; Ito, S.; Haque, S. A.; Torres, T.; Nüesch, F.; Geiger, T.; Zakeeruddin, S. M.; et al. PbS and CdS Quantum Dot-Sensitized Solid-State Solar Cells: "Old Concepts, New Results.". *Adv. Funct. Mater.* **2009**, *19*, 2735−2742.

(12) Harris, R. D.; Bettis Homan, S.; Kodaimati, M.; He, C.; Nepomnyashchii, A. B.; Swenson, N. K.; Lian, S.; Calzada, R.; Weiss, E. A. Electronic Processes within Quantum Dot-Molecule Complexes. *Chem. Rev.* **2016**, *116*, 12865−12919.

(13) Dayal, S.; Lou, Y.; Samia, A. C. S.; Berlin, J. C.; Kenney, M. E.; Burda, C. Observation of Non-Förster-Type Energy-Transfer Behavior in Quantum Dot−Phthalocyanine Conjugates. *J. Am. Chem. Soc.* **2006**, *128*, 13974−13975.

(14) Dworak, L.; Matylitsky, V. V.; Ren, T.; Basché, T.; Wachtveitl, J. Acceptor Concentration Dependence of Förster Resonance Energy Transfer Dynamics in Dye−Quantum Dot Complexes. *J. Phys. Chem. C* **2014**, *118*, 4396−4402.

(15) Sadhu, S.; Tachiya, M.; Patra, A. A Stochastic Model for Energy Transfer from CdS Quantum Dots/Rods (Donors) to Nile Red Dye (Acceptors). *J. Phys. Chem. C* **2009**, *113*, 19488−19492.

(16) Gopi, A.; Lingamoorthy, S.; Soman, S.; Yoosaf, K.; Haridas, R.; Das, S. Modulating FRET in Organic−Inorganic Nanohybrids for Light Harvesting Applications. *J. Phys. Chem. C* **2016**, *120*, 26569−26578.

(17) Beane, G.; Boldt, K.; Kirkwood, N.; Mulvaney, P. Energy Transfer between Quantum Dots and Conjugated Dye Molecules. *J. Phys. Chem. C* **2014**, *118*, 18079−18086.

(18) Drozdek, S.; Szeremeta, J.; Lamch, L.; Nyk, M.; Samoc, M.; Wilk, K. A. Two-Photon Induced Fluorescence Energy Transfer in Polymeric Nanocapsules Containing $CdSe_xS_{1−x}$/ZnS Core/Shell Quantum Dots and Zinc(II) Phthalocyanine. *J. Phys. Chem. C* **2016**, *120*, 15460−15470.

(19) Tkachenko, N. V. Photoinduced Charge Separation in Semiconductor-Quantum-Dot/Organic-Molecule Hybrids. *ChemPhotoChem* **2018**, *2*, 112−120.

(20) Clapp, A. R.; Medintz, I. L.; Mattoussi, H. Förster Resonance Energy Transfer Investigations Using Quantum-Dot Fluorophores. *ChemPhysChem* **2006**, *7*, 47−57.

(21) Kundu, S.; Patra, A. Nanoscale Strategies for Light Harvesting. *Chem. Rev.* **2017**, *117*, 712−757.

(22) Chou, K.; Dennis, M. A. Förster Resonance Energy Transfer between Quantum Dot Donors and Quantum Dot Acceptors. *Sensors* **2015**, *15*, 13288−13325.

(23) Boulesbaa, A.; Huang, Z.; Wu, D.; Lian, T. Competition between Energy and Electron Transfer from CdSe QDs to Adsorbed Rhodamine B. *J. Phys. Chem. C* **2010**, *114*, 962−969.

(24) Ragoussi, M.-E.; Ince, M.; Torres, T. Recent Advances in Phthalocyanine-Based Sensitizers for Dye-Sensitized Solar Cells. *Eur. J. Org. Chem.* **2013**, *2013*, 6475−6489.

(25) Martín-Gomis, L.; Fernandez-Lazaro, F.; Sastre-Santos, A. Advances in Phthalocyanine-Sensitized Solar Cells (PcSSCs). *J. Mater. Chem. A* **2014**, *2*, 15672−15682.

(26) Martínez-Díaz, M. V.; de la Torre, G.; Torres, T. Lighting Porphyrins and Phthalocyanines for Molecular Photovoltaics. *Chem. Commun.* **2010**, *46*, 7090−7108.

(27) Blas-Ferrando, V. M.; Ortiz, J.; Gonzalez-Pedro, V.; Sanchez, R. S.; Mora-Sero, I.; Fernandez-Lazaro, F.; Sastre-Santos, A. Efficient Passivated Phthalocyanine-Quantum Dot Solar Cells. *Chem. Commun.* **2015**, *51*, 1732−1735.

(28) Allen, C. M.; Sharman, W. M.; Van Lier, J. E. Current Status of Phthalocyanines in the Photodynamic Therapy of Cancer. *J. Porphyrins Phthalocyanines* **2001**, *5*, 161−169.

(29) Anula, H. M.; Berlin, J. C.; Wu, H.; Li, Y.-S.; Peng, X.; Kenney, M. E.; Rodgers, M. A. J. Synthesis and Photophysical Properties of Silicon Phthalocyanines with Axial Siloxy Ligands Bearing Alkylamine Termini. *J. Phys. Chem. A* **2006**, *110*, 5215−5223.

(30) Lobo, A. C. S.; Silva, A. D.; Tomé, V. A.; Pinto, S. M. A.; Silva, E. F. F.; Calvete, M. J. F.; Gomes, C. M. F.; Pereira, M. M.; Arnaut, L. G. Phthalocyanine Labels for Near-Infrared Fluorescence Imaging of Solid Tumors. *J. Med. Chem.* **2016**, *59*, 4688−4696.

(31) Britton, J.; Antunes, E.; Nyokong, T. Fluorescence Quenching and Energy Transfer in Conjugates of Quantum Dots with Zinc and Indium Tetraamino Phthalocyanines. *J. Photochem. Photobiol., A* **2010**, *210*, 1−7.

(32) Dayal, S.; Li, J.; Li, Y.-S.; Wu, H.; Samia, A. C. S.; Kenney, M. E.; Burda, C. Effect of the Functionalization of the Axial Phthalocyanine Ligands on the Energy Transfer in QD-Based Donor−Acceptor Pairs. *Photochem. Photobiol.* **2008**, *84*, 243−249.

(33) Blas-Ferrando, V. M.; Ortiz, J.; González-Pedro, V.; Sánchez, R. S.; Mora-Seró, I.; Fernández-Lázaro, F.; Sastre-Santos, Á. Synergistic Interaction of Dyes and Semiconductor Quantum Dots for Advanced Cascade Cosensitized Solar Cells. *Adv. Funct. Mater.* **2015**, *25*, 3220−3226.

(34) Arvani, M.; Virkki, K.; Abou-Chahine, F.; Efimov, A.; Schramm, A.; Tkachenko, N. V.; Lupo, D. Photoinduced Hole Transfer in QD−Phthalocyanine Hybrids. *Phys. Chem. Chem. Phys.* **2016**, *18*, 27414−27421.

(35) Zhu, H.; Song, N.; Lian, T. Controlling Charge Separation and Recombination Rates in CdSe/ZnS Type I Core−Shell Quantum Dots by Shell Thicknesses. *J. Am. Chem. Soc.* **2010**, *132*, 15038−15045.

(36) Lakowicz, J. R. *Principles of Fluorescence Spectroscopy*, 3rd ed.; Kluwer Academic/Plenum Publishers: New York, 1999; p 496.

(37) Morris-Cohen, A. J.; Frederick, M. T.; Cass, L. C.; Weiss, E. A. Simultaneous Determination of the Adsorption Constant and the Photoinduced Electron Transfer Rate for a Cds Quantum Dot−Viologen Complex. *J. Am. Chem. Soc.* **2011**, *133*, 10146−10154.

(38) Virkki, K.; Demir, S.; Lemmetyinen, H.; Tkachenko, N. V. Photoinduced Electron Transfer in CdSe/ZnS Quantum Dot−Fullerene Hybrids. *J. Phys. Chem. C* **2015**, *119*, 17561−17572.

(39) Wong, K. F.; Bagchi, B.; Rossky, P. J. Distance and Orientation Dependence of Excitation Transfer Rates in Conjugated Systems: Beyond the Förster Theory. *J. Phys. Chem. A* **2004**, *108*, 5752−5763.

(40) Shaw, P. E.; Ruseckas, A.; Samuel, I. D. W. Distance Dependence of Excitation Energy Transfer between Spacer-Separated Conjugated Polymer Films. *Phys. Rev. B* **2008**, *78*, No. 245201.

(41) Cid, J.-J.; Yum, J.-H.; Jang, S.-R.; Nazeeruddin, M. K.; Martínez-Ferrero, E.; Palomares, E.; Ko, J.; Grätzel, M.; Torres, T. Molecular Cosensitization for Efficient Panchromatic Dye-Sensitized Solar Cells. *Angew. Chem., Int. Ed.* **2007**, *46*, 8358−8362.

(42) Cid, J.-J.; García-Iglesias, M.; Yum, J.-H.; Forneli, A.; Albero, J.; Martínez-Ferrero, E.; Vázquez, P.; Grätzel, M.; Nazeeruddin, M. K.; Palomares, E.; et al. Structure−Function Relationships in Unsymmetrical Zinc Phthalocyanines for Dye-Sensitized Solar Cells. *Chem. - Eur. J.* **2009**, *15*, 5130−5137.

(43) García-Iglesias, M.; Cid, J.-J.; Yum, J.-H.; Forneli, A.; Vazquez, P.; Nazeeruddin, M. K.; Palomares, E.; Gratzel, M.; Torres, T. Increasing the Efficiency of Zinc-Phthalocyanine Based Solar Cells through Modification of the Anchoring Ligand. *Energy Environ. Sci.* **2011**, *4*, 189−194.